ISSN 0967-0912, Steel in Translation, 2012, Vol. 42, No. 6, pp. 544–547. © Allerton Press, Inc., 2012.
Original Russian Text © A.T. Kanaev, A.V. Bogomolov, T.E. Sarsembaeva, 2012, published in "Stal'," 2012, No. 6, pp. 58–61.

Improving the Wear Resistance of Wheel-Pair Rims by Plasma Quenching

A. T. Kanaev[a], A. V. Bogomolov[b], and T. E. Sarsembaeva[a]

[a] *Seifullin Kazakh Agrotechnology University, Astana, Kazakhstan*
[b] *Toraigyrov Pavlodar State University, Pavlodar, Kazakhstan*

Abstract—The formation of microstructure and substructures in the rims of railroad wheel pairs by plasma treatment is investigated. The hardening of the surface layer in plasma quenching is largely due to the formation of nonequilibrium metastable structure that is practically amorphous in the surface zone. This structure is transformed to a narrow zone of complete and incomplete quenching, with a nonuniform martensite + troostite structure.

DOI: 10.3103/S0967091212060083

Plasma surface treatment is an effective and productive method of increasing the wear resistance of steel parts. The heating prior to quenching is by means of a high-enthalpy plasma jet moving along the surface in the opposite direction to the moving part. The hot zone is cooled immediately on leaving the plasma, mainly on account of heat transfer into the massive steel part and convective heat transfer from the surface [1].

We investigate the rims of wheel pairs in the locomotive repair depot at Ust'-Kamenogorsk, which are manufactured from Ст2 steel in accordance with State Standard GOST 398–96. The steel contains 0.57–0.65% C, 0.22–0.45% Si, 0.60–0.90% Mn, ≤0.15% V, ≤0.035% P, and ≤0.040% S. The elevated carbon content (0.57–0.65%) ensures wear resistance and contact strength, on the one hand, and reduces the thermal stability, on the other. Therefore, vanadium is introduced in the steel, so as to increase the thermal stability.

The thermal conductivity of the material plays an important role in plasma heating, which involves energy supply to the surface and its conductive transfer to the interior of the metal. Microvolumes at different distances from the surface are heated to different temperatures; the heating and cooling rates of these microvolumes will also be different. Hence, control of plasma surface quenching entails determination of the temperature and time parameters in the thermal-influence zone during the heating stage.

In the subsequent cooling stage, the austenite formed in different temperature conditions breaks down. Establishing the types of structure in the thermal-influence zone and the corresponding properties entails determination of the cooling rate within the thermal-influence zone and its comparison with the thermokinetic decomposition curves of austenite at a certain austenite concentration and maximum temperature prior to quenching.

Note that, in plasma quenching, the absolute magnitude of the heat flux is 106–108 W/m^2. The thermal cycle of the process, consisting of a heating stage (length 1.0–1.2 s) and a cooling stage (1.5–2.0 s), lasts 2.5–3.0 s. The heating rate of the steel may reach $\geq 1.5 \times 10^3$ K/s.

The preliminary heat treatment of the rims involves quenching and subsequent tempering. The mechanical properties of the heat-treated rims are as follows: strength $\sigma_B = 930$–1100 N/mm^2; hardness $HB \geq 269$; impact strength $KCU = 25$ J/cm^2; hardness at the tip $HB \leq 321$. However, the first quality certificates for wheel rims did not indicate the conditions of strengthening heat treatment, although all the corresponding temperature parameters must be recorded, according to State Standard GOST 398–96, since the uniformity and dispersity of the initial structure may be judged on the basis of the heat treatment—in particular, the temperature and duration of tempering. This is important because the initial structure affects not only the structure formation in plasma treatment but also the depth of the hardened layer. In fact, different initial structure will be associated with different thermal conductivity, on account of the difference in the internal boundary surface between the ferrite and the carbide (cementite). Metallographic data show that the steel in the rim sent for plasma treatment contains a ferrite grid, which should not be observed in the quenched and tempered initial structure. That is indirect evidence of nonstandard heat treatment. In the sharp intense heating associated with plasma quenching, the increase in heat flux from the high-temperature jet to the treated surface must correspond to its thermophysical properties. The thermal diffusivity of steel 60 (an analog of Ст2 steel, which is investigated in the present work) is 0.13 cm^2/s at room temperature and declines to 0.05 cm^2/s at 1400°C [2, 3].

Table 1. Microhardness over the depth of the quenched zone

Initial microhardness *HV*	Surface plasma quenching			
	distance below surface, μm	microhardness of quenched zone *HV*		
		micromelting zone	transition zone	zone of initial structure
404.3	123	1380.3	–	–
404.9	300	1589.1	–	–
403.6	645.1	–	1021.5	–
–	932.5	–	1012.9	–
–	993.1	–	820.3	–
–	1120.3	–	662.7	–
–	1221.3	–	443.2	–
–	1239.4	–	–	404.6
–	1401.6	–	–	404.9

The high-temperature jet is generated by means of an electric-arc plasmatron based on protective gas. The gap between the plasmatron's nozzle aperture and the treated surface will depend on the plasmatron power and the required hardening depth. The plasma-treatment conditions are as follows: current 275 A; arc voltage 120 V; rated arc power 35 kW; protective-gas consumption 5 L/min; speed of wheel pair 0.143 rpm (7.0–7.2 min per complete wheel revolution).

The transition zone from the working surface to the contact surface (width 25–26 mm) is hardened. After plasma treatment, the surface layer is subjected to microstructural analysis; chemical composition of all the zones over the cross section is determined; the microhardness is determined over the depth of the hardened layer; and the thickness of the quenched layer is measured on a JEOL ISM-5910 raster electron microscope and a Leica Microsystems optical microscope. The microhardness is determined by the Vickers method on an inverted Leica Microsystems microscope, with a 2.5-N load.

The microhardness distribution over the depth of the quenched zone (in the first series of experiments) shows that the microhardness is a maximum at a distance of 124 μm from the surface: *HV* 1688.2. With increase in the depth, the microhardness declines, to *HV* 1000.8 at a depth of 921 μm and $HV \leq 413$ at a depth of 1175.9 μm. Table 1 presents the results of the second series of experiments.

Metallographic data for the hardened steel show that three zones of different microstructure may be distinguished over the depth.

(1) The micromelting zone, consisting of nonuniform finely disperse (near-amorphous) structure. The microstructure consists of a white nonetching layer of exceptionally high hardness (*HV* 1688.2 and *HV* 1589.1). This zone is nonuniform over the width of the treated surface: the maximum depth of 921 μm is seen in the central section; at the edge of the hardened layer, it is 148 μm (Fig. 1).

(2) The plasma-treatment zone, which is directly below the white nonetching layer and bounded by the incomplete-quenching zone (between critical points A_3 and A_1). The microhardness of this zone is typical of finely acicular martensite and troostomartensite. This is the transition zone to tempering sorbite more closely resembling the initial structure (Fig. 2).

(3) The zone of initial structure. This zone consists of finely disperse tempering sorbite with microhardness *HV* 400–450 (Fig. 3).

It follows from these experimental data that optimal plasma treatment is associated with reduced hardness and brittleness of the quenched zone. The thickness of the hardened layer and the hardness over its depth are monitored on samples cut from the wheel rim, in diametrically opposite directions.

Tests show that the wear resistance of the wheel pair's rims may be increased by forming finely disperse martensite structure with hardness *HV* 810–870 in the surface layer, characterized by smooth variation over the quenched zone. This may be accomplished, for example, by adjusting the angle at which the jet encounters the surface, so as to correct the heating and

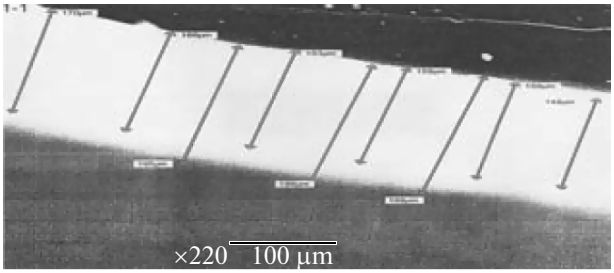

Fig. 1. Micromelting zone over the width of the treated surface (edge).

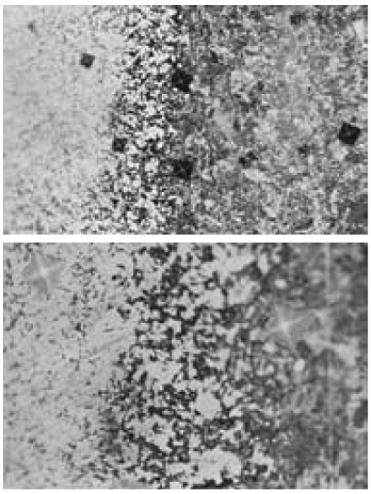

Fig. 2. Transition zone from amorphous to crystalline structure: (a) *HV* 1012.9, ×200; (b) *HV* 820.3, ×500.

cooling conditions in the rims; and by adjusting the wheel speed and the distance from the burners to the surface. Thus, in optimal treatment, the microhardness may be reduced so as to comply with Technical Specifications TU 0943-011-24328–98 (*HV* 801.9), with a structure corresponding to finely disperse martensite mixed with upper and lower bainite at a depth of 0.057–0.086 mm. Beyond the strengthened layer, the structure consists of troostite or troostosorbite with *HV* 609.46 (extending over 0.89–1.02 mm). The initial structure in the core (microhardness *HV* 324.59) consists of a mixture of ferrite and pearlite, with different degrees of dispersity.

Note that the microstructure observed after plasma treatment may be explained in terms of the superfast heating and subsequent cooling as the heat is transferred to cold layers of the metal. Correspondingly, the structural and phase components of the steel after plasma treatment are characterized by greater dispersity and higher internal phase stress (of types 2 and 3), as well as distinct chemical microheterogeneity. These findings are verified by special experiments to determine the chemical composition of the steel, with spark

Table 2. Results of multifractal analysis of images of the steel surface

Multifractal parameters	Layer		Initial structure
	hardened layer	transition layer	
Specific entropy S_{sp}	0.05	0.05	0.05
Degree of order Δ	0.143	0.082	0.115
Fractal dimensionality D_0	1.991	1.993	1.993
Uniformity R^2	0.922	0.986	0.936

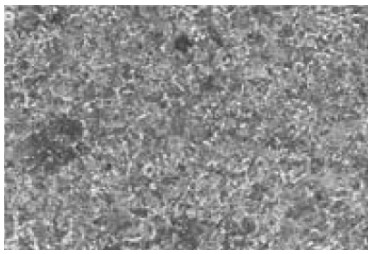

Fig. 3. Zone of initial structure (hardness *HV* 404); ×200.

spectral excitation in a Leica Microsystems Spectrolab JrCCD spectrometer. Chemical analysis over the depth of the plasma-treated and untreated zones confirms the chemical microheterogeneity of the structural and phase components in the steel.

The carbon content varies from 0.002 to 0.06 at % over the depth of the hardened zone. Other impurities (Si, Mn, P, etc.) are characterized by the same microheterogeneity over the depth of the hardened zone. This may be attributed to incomplete diffusion in high-speed heat treatment. In high-speed heating ($\geq 1.5 \times 10^3$ K/s), decarburization is practically impossible.

In the thermal cycle of plasma quenching, consisting of a heating stage (length 1.0–1.2 s) and a cooling stage (1.5–2.0 s), homogenization of the solid solution is incomplete within individual grains. This facilitates the formation of very hard metastable structures, with good wear resistance and microbinding in friction.

The nonuniformity and distortion of the structural and phase components may be confirmed by multifractal analysis of images of the steel surface. The results are summarized in Table 2.

It follows from Table 2 that the core has a relatively ordered nonuniform structure, evidently due to the preliminary heat treatment of the steel. The transition zone has a chaotic structure, which is very disorderly and uniform. The hardened layer with an elevated density of fractal components may be characterized as a multifractal structure, which is nonuniform and ordered. Since the fractal dimensionality $D_0 \approx 2$, the structure consists of close-packed clusters with fractal boundaries [4].

As already noted, if the initial structure consists of ferrite lattices around pearlite colonies, short-term plasma quenching does not completely homogenize the solid solution (austenite), and the layer quenched from the austenite state contains not only the martensite formed at the site of the former pearlite colonies but also ferrite lattices. With an initial structure that has been quenched and tempered, the ferrite lattice is absent. That facilitates smooth conversion of the quenching zone to a tempering zone with highly disperse troostite–sorbite structure. The formation of an extended troostite–sorbite structure (*HV* 609.46) between the hardened layer (*HV* 801.90) and the core

(*HV* 324.59) increases the crack resistance and reduces the compressive stress on the external layer. This transition zone slows the cracks formed in the brittle, hardened, plasma-quenched layer. This corresponds to smooth variation in the structure and microhardness over the depth of the hardened zone. We may suppose that this is also associated with decrease in tensile stress in the transition zone; in the quenched zone, the compressive stress is 250–350 MPa [2, 5].

Thus, the appearance of large compressive stress in the quenched surface layer and the decrease in tensile stress in the transition zone improve the reliability and durability of wheel rims under contact–fatigue loads.

CONCLUSIONS

(1) We have investigated the structure formation in plasma-treated rims of railroad wheel pairs. Optimal hardening in plasma quenching is due to the formation of disperse martensite structure with hardness *HV* 810–870 in the surface layer.

(2) The formation of an extended troostite–sorbite structure of intermediate hardness between the hardened layer and the unhardened core prevents lamination, increases the crack resistance, and reduces the compressive stress in the external layer.

(3) On plasma quenching, the structure formed by micromelting of a thin surface layer, with subsequent sharp cooling, is practically amorphous and is characterized by exceptionally high microhardness and great brittleness. Further from the surface, we note a zone with martensite structure and an incomplete-quenching region, with nonuniform troostite.

REFERENCES

1. Lykov, A.K., Red'kin, Yu.G., and Glibina, L.A., Methods of Plasma Quenching, *Lokomotiv*, 2000, no. 1, pp. 27–28.
2. Kanaev, A.T., Kusainova, K.T., and Toktanaeva, A.A., Plasma Hardening of Wheel-Pair Rims, *Vestn. Kaz. Akad. Transporta Kommun.*, 2004, no. 6(31), pp. 25–28.
3. Kanaev, A.T. and Kusainova, K.T., Influence of Plasma Hardening on the Structure of Wheel-Pair Rims, *Lokomotiv*, 2006, no. 6, pp. 59–63.
4. Ivanova, V.S., Balankin, A.S., Bunin, I.Zh., and Oksogoev, A.A., *Sinergetika i fraktaly v materialovedenii* (Synergetics and Fractals in Materials Science), Moscow: Nauka, 1995.
5. Kanaev, A.T. and Baibosynova, L.A., Structural Features and Chemical Composition of Strength over the Depth of Wheel-Pair Rims after Plasma Hardening, *Materialy V Mezhdunar. nauch.-prakt. konferentsii Noveishie nauchnye dostizheniya-2009* (Proceedings of Fifth International Conference on New Scientific Developments), Sofiya: Byal Grad-BI, 2009, vol. 24, pp. 3–6.